

# Determination of Rate Constants for the Activation Step in Atom Transfer Radical Polymerization Using the Stopped-Flow Technique

Tomislav Pintauer,<sup>†</sup> Wade Braunecker,<sup>†</sup>  
Edmond Collange,<sup>‡</sup> Rinaldo Poli,<sup>\*,§</sup> and  
Krzysztof Matyjaszewski<sup>\*,†</sup>

Department of Chemistry, Carnegie Mellon University,  
4400 Fifth Avenue, Pittsburgh, Pennsylvania 15213;  
Laboratoire de Synthèse et d'Electrosynthèse  
Organométalliques, Faculté des Sciences "Gabriel",  
Université de Bourgogne, 6 Boulevard Gabriel, 21000 Dijon,  
France; and Laboratoire de Chimie de Coordination, 205  
Route de Narbonne, 31077 Toulouse Cedex, France

Received October 30, 2003

Revised Manuscript Received March 8, 2004

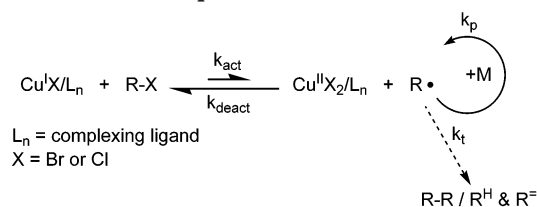
The synthesis of macromolecules with well-defined compositions, architectures, and functionalities represents an ongoing effort in the field of polymer chemistry. Over the past few years, atom transfer radical polymerization (ATRP) has emerged as a very powerful and robust technique to meet these goals.<sup>1–3</sup> The basic working mechanism of ATRP (Scheme 1) involves a reversible switching between two oxidation states of a transition metal complex.<sup>4,5</sup> Typically, copper(I) halide is used in conjunction with a nitrogen-based complexing ligand.<sup>4,6–9</sup>

Homolytic cleavage of the alkyl halogen bond (R–X) by Cu<sup>I</sup>X/L<sub>n</sub> generates an alkyl radical R• and the corresponding Cu<sup>II</sup>X<sub>2</sub>/L<sub>n</sub> complex. The radical R• can propagate with a rate constant *k<sub>p</sub>*, by adding to the double bond of a vinyl monomer, terminate by either coupling or disproportionation (*k<sub>t</sub>*), or be reversibly deactivated by the Cu<sup>II</sup>X<sub>2</sub>/L<sub>n</sub> complex (*k<sub>deact</sub>*). Radical termination is diminished as a result of the persistent radical effect,<sup>10</sup> and the equilibrium is strongly shifted toward the dormant species (*k<sub>act</sub>* ≪ *k<sub>deact</sub>*). Consequently, polymers with predictable molecular weights, narrow molecular weight distributions, and high functionalities have been synthesized.<sup>11–16</sup>

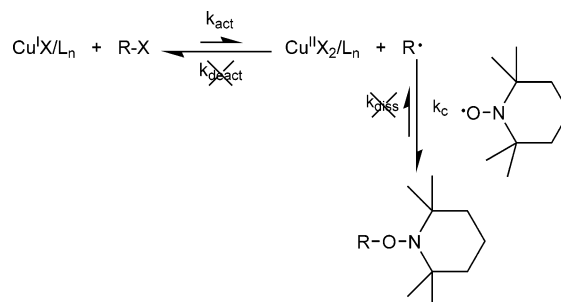
Fundamental studies are crucial to future developments in the ATRP. Factors that deserve consideration in such a study include the determination of the rate constants of elementary reactions occurring in the ATRP such as activation, deactivation, and initiation.<sup>17–25</sup> Even more important is the correlation of these rate constants with such reaction parameters as catalyst, alkyl halide and monomer structure, temperature, and solvent.<sup>26–29</sup> These investigations can potentially optimize the development of catalysts for particular monomers and reaction conditions and generally improve the overall catalytic process.

In this paper, we report the use of stopped-flow techniques to measure very fast activation rate constants for model systems in copper-mediated ATRP which were previously not investigated due to the limitations in current methods which are mostly based on NMR and GC measurements. Furthermore, the

Scheme 1. Proposed Mechanism for ATRP



Scheme 2. Kinetic Isolation of the Activation Process in the ATRP



activation parameters for some of the model systems are reported.

Activation rate constants (*k<sub>act</sub>*) in the ATRP are typically determined from model studies in which the transition metal complex is reacted with alkyl halide in the presence of radical trapping agents such as TEMPO.<sup>18,19,30</sup> The rates are typically determined by monitoring the rate of disappearance of the alkyl halide in the presence of excess activator (Cu<sup>I</sup>X/L<sub>n</sub>) and excess TEMPO which traps radicals faster than Cu<sup>II</sup>X<sub>2</sub>/L<sub>n</sub>.<sup>18,31–34</sup> Under such conditions, the activation rate constant can be kinetically isolated from the deactivation rate constant and is given by  $\ln([\text{RX}]_0/[\text{RX}]_t) = -k_{\text{act}}[\text{Cu}^{\text{I}}\text{X}/\text{L}_n]_0 t$  (Scheme 2).<sup>18</sup> The values were also determined for some polymeric systems using GPC techniques and similar kinetic expressions.<sup>20</sup> However, both methods are limited in measuring fast rate constants with the maximum upper limit of approximately 2 M<sup>–1</sup> s<sup>–1</sup>. This prompted us to consider the stopped-flow technique for measuring very fast activation rate constants for model systems in copper-mediated ATRP, since the mixing time (ca. 1 ms) and speed of data collection (one full spectrum every ca. 1 ms for diode-array UV–vis spectrophotometers) allow the measurement of pseudo-first-order rate constants up to ca. 1.5 × 10<sup>2</sup> s<sup>–1</sup> (*t*<sub>1/2</sub> = ca. 5 ms). The structures of model alkyl halides and complexing ligands used in conjunction with Cu<sup>I</sup>Br or Cu<sup>I</sup>Cl are shown in Scheme 3. In addition, ligands such as pyridineimines,<sup>35</sup> picolylamines,<sup>36</sup> cyclic amines,<sup>37</sup> and phenanthrolines<sup>38</sup> have also been used.

The activation rate constants were determined in CH<sub>3</sub>CN at variable temperatures using previously reported experimental procedures<sup>18</sup> with the exception that an excess of alkyl halide (RX) and TEMPO were used, and the rates were determined by monitoring the disappearance of the copper complex according to  $\ln([\text{Cu}^{\text{I}}\text{X}/\text{L}_n]_0/[\text{Cu}^{\text{I}}\text{X}/\text{L}_n]_t) = k_{\text{obs}} t = -k_{\text{act}}[\text{RX}]_0 t$ . Typically, 10–25 equiv of RX and TEMPO relative to the starting Cu<sup>I</sup>X/L<sub>n</sub> complex were used, with  $[\text{Cu}^{\text{I}}\text{X}/\text{L}_n]_0 = 1.0 \times 10^{-3}$ – $3.0 \times 10^{-3}$  M. The kinetic runs were carried out with a Hitech SF-61-DX2 apparatus equipped with a 1

<sup>†</sup> Carnegie Mellon University.

<sup>‡</sup> Université de Bourgogne.

<sup>§</sup> Laboratoire de Chimie de Coordination.

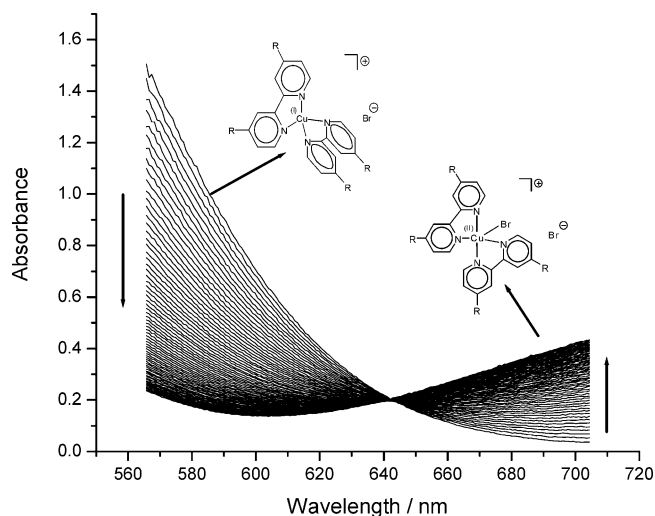
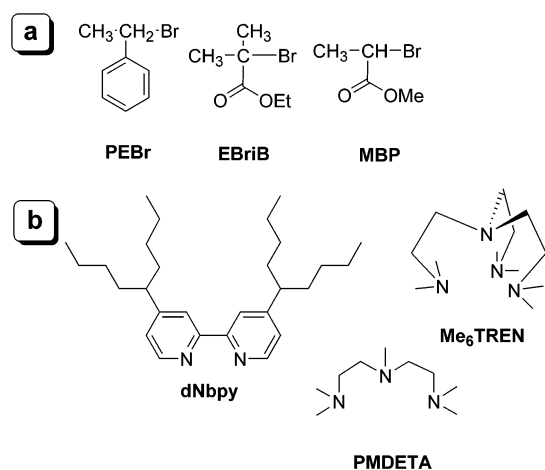


**Figure 1.** Time-dependent absorption spectra of  $\text{Cu}^{\text{I}}\text{Br}/2\text{dNbpy}$  in the presence of  $\text{EBriB}$  in  $\text{CH}_3\text{CN}$  at  $25\text{ }^\circ\text{C}$ .  $[\text{Cu}^{\text{I}}\text{Br}/2\text{dNbpy}]_0:[\text{EBriB}]_0:[\text{TEMPO}]_0 = 1:20:20$ ,  $[\text{Cu}^{\text{I}}\text{Br}/2\text{dNbpy}]_0 = 2.7 \times 10^{-3}\text{ M}$ , spectra recorded every 1 s ( $t_{\text{start}} = 0.5\text{ s}$ ,  $t_{\text{end}} = 70.5\text{ s}$ ).

**Scheme 3. Structures of Model Compounds (a) and Complexing Ligands (b) Used in the Activation Studies**



cm quartz cell and coupled with a Hitech diode-array UV-vis spectrophotometer. Such an excess amount of TEMPO was found sufficient to ensure a complete radical trapping and the total suppression of the deactivation process (see Scheme 2). These conditions were chosen primarily because of the strong interference of TEMPO in the UV region of the absorption spectra which does not enable the determination of the concentrations of alkyl halide accurately. The observed rate constant ( $k_{\text{obs}} = k_{\text{act}}[\text{RX}]_0$ ) and reaction order were determined using the commercially available SpecFit program.<sup>39</sup>

Shown in Figure 1 is the typical time-dependent absorption spectra recorded for the reaction of  $\text{Cu}^{\text{I}}\text{Br}/2\text{dNbpy}$  in the presence of excess  $\text{EBriB}$  and TEMPO in  $\text{CH}_3\text{CN}$  at  $25\text{ }^\circ\text{C}$ . As indicated in Figure 1, during the progress of the reaction the decrease of the absorption spectra in the 400–650 nm region is accompanied by a corresponding increase in the 650–800 nm region. The latter indicates the formation of the  $\text{Cu}^{\text{II}}\text{Br}_2/2\text{dNbpy}$  complex whose spectrum has been fully characterized.<sup>40–42</sup> Data analysis performed using the SpecFit program indicated first-order reaction conditions with observed rate constant of  $k_{\text{obs}} = 0.053\text{ s}^{-1}$ , from which

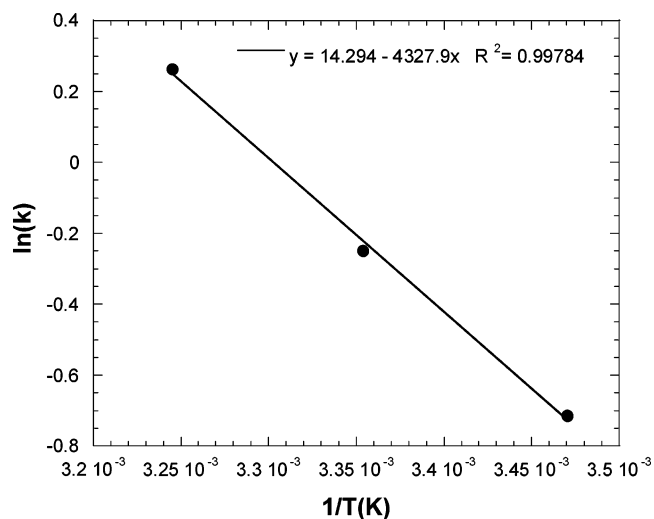


**Figure 2.** Arrhenius plot for the reaction between  $\text{Cu}^{\text{I}}\text{Br}/2\text{dNbpy}$  and  $\text{EBriB}$  in  $\text{CH}_3\text{CN}$  (experimental conditions are given in Figure 1).

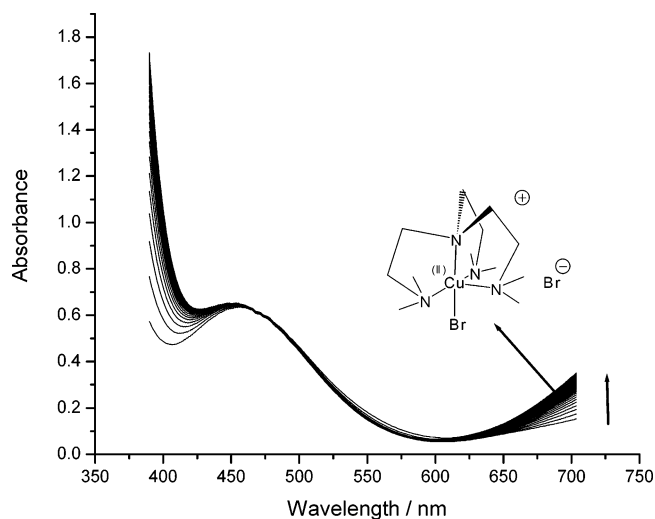


**Figure 3.** Time-dependent absorption spectra of  $\text{Cu}^{\text{I}}\text{Br}/\text{Me}_6\text{TREN}$  in the presence of  $\text{PEBr}$  in  $\text{CH}_3\text{CN}$  at  $15\text{ }^\circ\text{C}$ .  $[\text{Cu}^{\text{I}}\text{Br}/\text{Me}_6\text{TREN}]_0:[\text{PEBr}]_0:[\text{TEMPO}]_0 = 1:20:20$ ,  $[\text{Cu}^{\text{I}}\text{Br}/\text{Me}_6\text{TREN}]_0 = 2.7 \times 10^{-3}\text{ M}$ , 160 scans, ( $t_{\text{start}} = 0.002\text{ s}$ ,  $t_{\text{end}} = 3.80\text{ s}$ ).

the activation rate constant was calculated as  $k_{\text{act}} = 0.78\text{ M}^{-1}\text{ s}^{-1}$ . Similarly, the rates at different temperatures can be used to determine the activation parameters,  $\Delta H^\ddagger$  and  $\Delta S^\ddagger$ , as shown in Figure 2. The advantage of the stopped-flow technique in terms of accessing very high reaction rates was first demonstrated in the case of relatively active  $\text{Cu}^{\text{I}}\text{Br}/\text{Me}_6\text{TREN}$  system and  $\text{PEBr}$  under pseudo-first-order reaction conditions in  $\text{CH}_3\text{CN}$  at  $15\text{ }^\circ\text{C}$  (Figure 3).

The activation rate constant for this system at  $25\text{ }^\circ\text{C}$  was determined to be  $k_{\text{act}} = 8.6 \times 10^2\text{ M}^{-1}\text{ s}^{-1}$ . A study of  $\text{Cu}^{\text{I}}\text{Br}/\text{Me}_6\text{TREN}$  and  $\text{MBP}$  under the same reaction conditions and temperature revealed a slightly more reactive system with  $k_{\text{act}} = 1.1 \times 10^3\text{ M}^{-1}\text{ s}^{-1}$ . While systems faster than these can still be measured using pseudo-first-order reaction conditions, more scans and hence more reliable data can be obtained using second-order conditions (i.e., stoichiometric amounts of  $\text{Cu}^{\text{I}}\text{X}/\text{L}_n$  complex and alkyl halide  $\text{RX}$ ). The activation rate constant for  $\text{Cu}^{\text{I}}\text{Br}/\text{Me}_6\text{TREN}$  and  $\text{EBriB}$  was determined under second-order conditions in  $\text{CH}_3\text{CN}$  at  $25\text{ }^\circ\text{C}$  as  $k_{\text{act}} = 7.7 \times 10^3\text{ M}^{-1}\text{ s}^{-1}$ , or approximately 10 000 times faster than the  $\text{Cu}^{\text{I}}\text{Br}/2\text{dNbpy}$  system under the

**Table 1. Summary of Activation Rate Constants in CH<sub>3</sub>CN for Various Copper(I) Complexes and Initiators Used in the ATRP As Determined Using the Stopped-Flow Technique**

complex	initiator	reaction order	<i>T</i> /°C	<i>k</i> <sub>act</sub> /M <sup>-1</sup> s <sup>-1</sup>	Δ <i>H</i> <sup>‡</sup> /kJ mol <sup>-1</sup> <sup>a</sup>	Δ <i>S</i> <sup>‡</sup> /J K <sup>-1</sup> mol <sup>-1</sup> <sup>a</sup>
Cu <sup>I</sup> Br/2dNbpy	EBriB	pseudo first	15	0.49 ± 0.01	33.5 ± 1.7	-134 ± 6
			25	0.78 ± 0.02		
			35	1.3 ± 0.05		
Cu <sup>I</sup> Br/PMDETA	EBriB	pseudo first	15	1.4 ± 0.03	38.9 ± 3.6	-107 ± 12
			25	2.3 ± 0.06		
			35	4.3 ± 0.07		
Cu <sup>I</sup> Br/Me <sub>6</sub> TREN	PEBr	pseudo first	5	(4.5 ± 0.2) × 10 <sup>2</sup>	20.3 ± 1.2	-120 ± 4
			15	(6.7 ± 0.2) × 10 <sup>2</sup>		
			25	(8.6 ± 0.3) × 10 <sup>2</sup>		
			35	(1.2 ± 0.3) × 10 <sup>3</sup>		
	EBriB	second	15	(5.7 ± 0.3) × 10 <sup>3</sup>	19.3 ± 3.1	-106 ± 11
			20	(6.9 ± 0.1) × 10 <sup>3</sup>		
			25	(7.7 ± 0.2) × 10 <sup>3</sup>		
	MBP	pseudo first	25	(1.1 ± 0.3) × 10 <sup>3</sup>		
			25	(1.1 ± 0.3) × 10 <sup>3</sup>		

<sup>a</sup> For fit index (*R*<sup>2</sup>) see Figure 2 and Supporting Information.

same experimental conditions. The activation rate constants and parameters (Δ*H*<sup>‡</sup> and Δ*S*<sup>‡</sup>), determined for the copper(I) complexes and alkyl halides in CH<sub>3</sub>CN, are summarized in Table 1.

The activation rate constants for Cu<sup>I</sup>Br/2dNbpy and Cu<sup>I</sup>Br/PMDETA systems are in good agreement with previously reported values using GC techniques.<sup>18,26,27,30</sup> Furthermore, the activation parameters for PEBR and EBriB using Cu<sup>I</sup>Br/2dNbpy, Cu<sup>I</sup>Br/PMDETA, and Cu<sup>I</sup>Br/Me<sub>6</sub>TREN complexes can now be used to calculate the corresponding activation rate constants at polymerization temperatures (*T* = 60–110 °C). While it has been shown that PEBR is a good model compound for a polystyrene chain end,<sup>20</sup> the same might not hold for EBriB and methyl methacrylate, due to the recently demonstrated penultimate effect.<sup>30</sup> These activation parameters for Cu<sup>I</sup>Br/Me<sub>6</sub>TREN that were previously unavailable, and the activation data for other highly reactive systems yet to be measured will be critical when modeling the kinetics of such polymerization systems.<sup>43</sup>

As indicated in Table 1, the activation rate constants for Cu<sup>I</sup>Br/Me<sub>6</sub>TREN are much higher than for Cu<sup>I</sup>Br/2dNbpy and Cu<sup>I</sup>Br/PMDETA complexes. This is reflected in their redox potentials, and our previous investigation of these systems indicated that Cu<sup>I</sup>Br/Me<sub>6</sub>TREN is a much more reducing catalyst.<sup>44</sup> We are also attempting to correlate the activation rate constant and the catalyst structure as well as exploring the determination of the deactivation rate constants via measurements of the overall equilibrium constant for ATRP (*K*<sub>ATRP</sub> = *k*<sub>act</sub>/*k*<sub>deact</sub>) using the persistent radical effect.

When the stopped-flow apparatus is set up on the benchtop, there is the potential for slow diffusion of oxygen through the apparatus to the sample. Monitoring the absorbance spectra of Cu<sup>I</sup>Br/2dNbpy in the apparatus for 1000 s in the absence of alkyl halide revealed the complex was slowly oxidized (<10%). This oxidation was not significant enough to affect the measurement of activation rate constants for Cu<sup>I</sup>Br/2dNbpy and EBriB because the reaction was complete long before significant diffusion of oxygen through the system could occur.

In conclusion, the stopped-flow technique was used to determine the activation rate constants in CH<sub>3</sub>CN at variable temperatures for alkyl halides and very active Cu<sup>I</sup>X/L<sub>*n*</sub> complexes, which were previously not accessible due to the limitations in measuring fast reaction rates with current GC and NMR techniques. The activation rate constants for EBriB were found to increase in the order Cu<sup>I</sup>Br/2dNbpy < Cu<sup>I</sup>Br/PMDETA

<< Cu<sup>I</sup>Br/Me<sub>6</sub>TREN. The rate constants of activation (*k*<sub>act</sub>) for PEBR (8.6 × 10<sup>2</sup> M<sup>-1</sup> s<sup>-1</sup>), MBP (1.1 × 10<sup>3</sup> M<sup>-1</sup> s<sup>-1</sup>), and EBriB (7.7 × 10<sup>3</sup> M<sup>-1</sup> s<sup>-1</sup>) at 25 °C for the Cu<sup>I</sup>Br/Me<sub>6</sub>TREN complex were found to be orders of magnitude higher than the corresponding Cu<sup>I</sup>Br/2dNbpy and Cu<sup>I</sup>Br/PMDETA complexes. The demonstrated effectiveness of the stopped-flow technique to measure fast reaction rates opens a new way to systematically determine activation rate constants and activation parameters for other highly active ATRP complexes.

**Acknowledgment.** The financial support from the CMU CRP Consortium and the NSF grant (CHE-0096601) is greatly appreciated. R.P. and E.C. thank the Conseil Régional de Bourgogne for funds that allowed the purchase of the stopped-flow apparatus.

**Supporting Information Available:** Detailed experimental procedures, Arrhenius plots for the determination of Δ*H*<sup>‡</sup> and Δ*S*<sup>‡</sup>, and time-dependent absorption spectra for alkyl halides and copper(I) complexes used in the study (PDF). This material is available free of charge via the Internet at <http://pubs.acs.org>

## References and Notes

- (1) Matyjaszewski, K.; Davis, T. P. *Handbook of Radical Polymerization*; John Wiley & Sons: Hoboken, 2002.
- (2) Matyjaszewski, K.; Xia, J. *Chem. Rev.* **2001**, *101*, 2921–2990.
- (3) Kamigaito, M.; Ando, T.; Sawamoto, M. *Chem. Rev.* **2001**, *101*, 3689–3745.
- (4) Wang, J.-S.; Matyjaszewski, K. *J. Am. Chem. Soc.* **1995**, *117*, 5614–5615.
- (5) Patten, T. E.; Xia, J.; Abernathy, T.; Matyjaszewski, K. *Science* **1996**, *272*, 866–868.
- (6) Matyjaszewski, K.; Patten, T. E.; Xia, J. *J. Am. Chem. Soc.* **1997**, *119*, 674–680.
- (7) Xia, J.; Matyjaszewski, K. *Macromolecules* **1997**, *30*, 7697–7700.
- (8) Xia, J.; Gaynor, S. G.; Matyjaszewski, K. *Macromolecules* **1998**, *31*, 5958–5959.
- (9) Xia, J.; Zhang, X.; Matyjaszewski, K. In *Transition Metal Catalysis in Macromolecular Design*; Boffa, L. S., Novak, B. M., Eds.; American Chemical Society: Washington, DC, 2000; Vol. 760, pp 207–223.
- (10) Fischer, H. *Chem. Rev.* **2001**, *101*, 3581–3610.
- (11) Coessens, V.; Pintauer, T.; Matyjaszewski, K. *Prog. Polym. Sci.* **2001**, *26*, 337–377.
- (12) Patten, T. E.; Matyjaszewski, K. *Acc. Chem. Res.* **1999**, *32*, 895–903.
- (13) Matyjaszewski, K. *Chem.—Eur. J.* **1999**, *5*, 3095–3102.
- (14) Patten, T. E.; Matyjaszewski, K. *Adv. Mater.* **1998**, *10*, 901–915.
- (15) Davis, K. A.; Matyjaszewski, K. *Adv. Polym. Sci.* **2002**, *159*, 30–106.

- (16) Pyun, J.; Matyjaszewski, K. *Chem. Mater.* **2003**, *13*, 3436–3448.
- (17) Pintauer, T.; Zhou, P.; Matyjaszewski, K. *J. Am. Chem. Soc.* **2002**, *124*, 8196–8197.
- (18) Matyjaszewski, K.; Paik, H.-j.; Zhou, P.; Diamanti, S. J. *Macromolecules* **2001**, *34*, 5125–5131.
- (19) Goto, A.; Fukuda, T. *Macromol. Rapid Commun.* **1999**, *20*, 633–636.
- (20) Ohno, K.; Goto, A.; Fukuda, T.; Xia, J.; Matyjaszewski, K. *Macromolecules* **1998**, *31*, 2699–2701.
- (21) Auke, S.; Klumperman, B.; Van der Linde, R. *Macromolecules* **2002**, *35*, 4785–4790.
- (22) Chambard, G.; Klumperman, B.; German, A. L. *Macromolecules* **2002**, *35*, 3420–3425.
- (23) Zhang, H.; Klumperman, B.; Ming, W.; Fischer, H.; van der Linde, R. *Macromolecules* **2001**, *34*, 6169–6173.
- (24) Chambard, G.; Klumperman, B.; German, A. L. *Macromolecules* **2002**, *35*, 3420–3425.
- (25) Yoshikawa, C.; Goto, A.; Fukuda, T. *Macromolecules* **2003**, *36*, 908–912.
- (26) Nanda, A. K.; Matyjaszewski, K. *Macromolecules* **2003**, *36*, 599–604.
- (27) Nanda, A. K.; Matyjaszewski, K. *Macromolecules* **2003**, *36*, 1487–1493.
- (28) Matyjaszewski, K.; Gobelt, B.; Paik, H.-j.; Horwitz, C. P. *Macromolecules* **2001**, *34*, 430–440.
- (29) Chambard, G.; Klumperman, B.; German, A. L. *Macromolecules* **2000**, *33*, 4417–4421.
- (30) Nanda, A. K.; Matyjaszewski, K. *Macromolecules* **2003**, *36*, 8222–8224.
- (31) Beckwith, A. L. J.; Bowry, V. W.; Ingold, K. U. *J. Am. Chem. Soc.* **1992**, *114*, 4983–4992.
- (32) Beckwith, A. L. J.; Bowry, V. W.; Moad, G. *J. Org. Chem.* **1988**, *53*, 1632–1641.
- (33) Chateaufneuf, J.; Luszyk, J.; Ingold, K. U. *J. Org. Chem.* **1988**, *53*, 1629–1632.
- (34) Gromada, J.; Matyjaszewski, K. *Macromolecules* **2002**, *35*, 6167–6173.
- (35) Haddleton, D. M.; Jasieczek, C. B.; Hannon, M. J.; Shooter, A. J. *Macromolecules* **1997**, *30*, 2190–2193.
- (36) Xia, J.; Matyjaszewski, K. *Macromolecules* **1999**, *32*, 2434–2437.
- (37) Teodorescu, M.; Matyjaszewski, K. *Macromolecules* **1999**, *32*, 4826–4831.
- (38) Destarac, M.; Bessiere, J. M.; Boutevin, B. *Macromol. Rapid Commun.* **1997**, *18*, 967–974.
- (39) Binstead, R. A.; Jung, B.; Zuberbühler, A. D. 2000 Spectrum Software Associates, Chapel Hill, NC, 2000.
- (40) Pintauer, T.; Qiu, J.; Kickelbick, G.; Matyjaszewski, K. *Inorg. Chem.* **2001**, *40*, 2818–2824.
- (41) Murphy, G.; O'Sullivan, C.; Murphy, B.; Hathaway, B. *Inorg. Chem.* **1998**, *37*, 240–248.
- (42) O'Sullivan, C.; Murphy, G.; Murphy, B.; Hathaway, B. *J. Chem. Soc., Dalton Trans.* **1999**, *11*, 1835–1844.
- (43) Gillies, M. B.; Matyjaszewski, K.; Norrby, P.-O.; Pintauer, T.; Poli, R.; Richard, P. *Macromolecules* **2003**, *36*, 8551–8559.
- (44) Qiu, J.; Matyjaszewski, K.; Thouin, L.; Amatore, C. *Macromol. Chem. Phys.* **2000**, *201*, 1625–1631.

MA035634F